

# Semi-autonomous shared control of large-scale manipulator arms

A. Hansson<sup>a</sup>, M. Servin<sup>b</sup>

<sup>a</sup>Umeå University, Umeå, Sweden.

<sup>b</sup>Umeå University, Umeå, Sweden (martin.servin@physics.umu.se).

---

## Abstract

Semi-autonomous operation with shared control between the human operator and control computer has been developed and examined for a large-scale manipulator for gripping and lifting heavy objects in unstructured dynamical environments. The technique has been implemented on a electro-hydraulic actuated crane arm with redundant kinematic structure. Several modes of automation and interaction were evaluated. Experiments show satisfactory smoothness in the transitions between autonomous, shared and manual control, doubled performance in log loading for inexperienced operators while experienced operators reported reduced workload.

*Keywords:* Autonomous control, Man/machine interaction, Human supervisory control, Large-scale redundant manipulator, Robotics in Agriculture and Forestry.

---

## 1. Introduction

Introducing automation in heavy machine operation is challenging from both research and engineering point-of-view. Large manipulator arms operated in unstructured (out-door) environment and in industrial applications is considered, e.g., forestry, construction, mining and off-shore operations. Among the typical work tasks are gripping, lifting and moving heavy objects. These manipulators are conventionally hydraulic actuated and with redundant kinematic structure. The challenges include accurate and robust tracking and control of joint motion, planning and execution of manipulator motions for different tasks, robust sensors, suitable interface to human operator and overall safe and robust system integration. Considering industrial applications the challenges also include high requirements on productivity and use of cost-efficient technology. The difficulties in joint motion control for a large hydraulic actuated manipulator arm include non-linear effects such as friction in valves, cylinders and joint axes, and complicated internal dynamics in the hydraulics system. Planning and execution of motion of manipulators in unstructured environment is complicated by that target objects and obstacles may appear in different shapes and at locations that vary dynamically, and operations may involve advanced motions that must be adjusted to the dynamical behavior of the objects, e.g., sorting of objects, pushing and pulling of objects, stabilization of swinging load. Control and automation typically requires continuous sensing of the state of the manipulator and its environment. In industrial out-door settings it might not be possible to find robust sensor solutions. A human operator can compensate for these deficiencies, e.g., making intelligent task planning and taking control over operations that require visual processing and motion correlation that is beyond current machine capability. As a consequence, most industrial manipulators in unstructured environments are operated manually by humans. Introducing semi-automation is motivated by the desire to improve productivity, cost efficiency

and the working condition for the human operators, that experience fatigue from the vast amount of information and decisions despite that most tasks are by routine operations. It is however very unclear how to design good interface between human operator and industrial manipulators that unloads the operator by autonomous execution of routine tasks without sacrificing overall productivity, safety and the fidelity of manual control. The purpose of the current paper is to provide a solution for shared control between human operators and industrial manipulators with semi-autonomous functionality in unstructured (out-door) environments that meets the relevant requirements.

As a particular platform for development and experimentation an electro-hydraulic actuated crane with an underactuated gripper is chosen, assumed to be mounted on a movable platform, e.g., a vehicle, and operated in dynamical unstructured environment. The results should also apply to many other setups of industrial manipulators with redundant kinematic chain structure. The particular industry application addressed is collection and loading of logs onto a terrain transportation vehicle at forest felling sites, a process known as *forwarding*. In northern Europe the most common machine system in final felling and thinning consist of one harvester and one forwarder. The harvester fells, delimits and bucks trees into logs. The forwarding task includes moving the vehicle over the terrain, approaching logs cut by the harvester, extracting the crane arm, gripping one or several logs, lifting them onto the load bunk of the forwarder machine where they are released and sorted by quality and species. After transportation through the terrain to the nearest road-side, logs are unloaded and sorted in piles of different quality and species. Figure 1 shows part of the forwarding task. In particular gripping, releasing and sorting may require human involvement while the other crane motions are more routine tasks and can be automatized. However, the positions of the logs, obstacles and the vehicle itself varies and in lack of reliable, cost-efficient solutions for out-door machine



Figure 1: Large-scale manipulator on forwarder machine (Valmet 860.4) loading logs at the felling site and unloading at the road side. Image courtesy of Komatsu Forest.

vision, the operator must be able to guide the system whenever necessary. Increased automation is strongly demanded by industry for reasons of increased productivity and improved operator work environment. The benefits for increased automation and teleoperation in heavy machine operation has been considered in Lapointe et al. (2001) and, with focus on forestry machines, in Hallonborg (2003) and in Brander et al. (2004).

A solution for shared control between human operator and computer control system of mechanical manipulator is presented. Shared control enables the human operator and the control computer to interact in the execution of pre-planned tasks with the manipulator arm, e.g., assist or intervene with each other to avoid risk-full actions, to adjust for variable or uncertain position of targets and obstacles or increased speed or precision when possible. The solution is aimed at meeting particular requirements relevant for industrial applications in unstructured (out-door) environment. These requirements include intuitive operation interface, not restricting experienced users in executing fast and precise maneuvers yet easy-to-learn for inexperienced operators, substantial unloading operator mental and physical stress during work, smooth transitions between manual and autonomous modes of operation. Since the operator and the environment is highly dynamical the automation system must be based on time-independent motion control. Given the size and strength of industrial manipulators safety is essential.

### 1.1. Previous and related work

Low-level control of hydraulic actuated large-scale manipulator arms with redundant kinematic structure have been considered in La Hera et al. (2008), and extended to optimal re-planning of motions in Mettin et al. (2009b) and Mettin et al. (2009a), and to teleoperation through virtual environment user interface in Westerberg et al. (2008). The present paper considered the very same manipulator platform and extends this series of work.

A variety of shared control systems are discussed in Sheridan (1992). A technique for simultaneous collaborative control of a small manipulator arm with the operator functionalities stop, speed-up, slow-down, move-orthogonal with respect to a pre-planned trajectory was presented in Tarn et al. (1996) together with experimental results. The combination of potential fields and constraints in limiting or guiding a human operator in controlling a manipulator was considered in Aigner and McCarragher (1997).

### 1.2. Our contribution

The main contribution of the present work is a solution for shared control between a human operator and computer control system in operating a large-scale manipulator for semi-autonomous operation in unstructured environment. The solution assumes robust joint control and path planner for the end-effector in cartesian space. Several modes of operation and with different level of automation are implemented on a particular electro-hydraulic redundant forestry crane and tested with experienced and inexperienced operators. Shared control is achieved by mixing the velocity references of the automation system for tracking a pre-planned motion with that of the operator generated velocity reference. This enables the human operator and the control computer to assist or intervene with each other in the execution of a manipulator task, e.g., to avoid risk-full actions, to adjust for variable or uncertain position of targets and obstacles or increased speed or precision when possible. Smooth transitions between autonomous, semi-autonomous and manual control is realized by giving the mixing coefficients specific functional dependency. The operator can chose between cartesian operation of the end-effector or conventional joint operation. Shared control in the latter mode is realized by converting the operator input signal to the corresponding cartesian operator end-effector velocity and making corresponding modification of the weight-factors in the inverse kinematics computation of the joint velocities from the mixed end-effector velocity. Experiments with human operators are designed to give relevant measures on the operator performance for the task of loading heavy objects with a large-scale manipulator with semi-autonomous shared control. In particular the experiment is designed for the task of forestry log loading.

## 2. Kinematics and motion control

Manipulators with redundant open chain kinematics are considered, where  $\theta = [\theta_1, \dots, \theta_n]^T$ ,  $n > m$  are the manipulator joints variables and  $m$  is the task space dimension. Positioning the end-effector in 3D cartesian space is considered, while the end-effector orientation control is not, i.e.  $m = 3$ . The end-effector orientation is assumed to be controlled by the operator although it is straightforward to automate (La Hera et al., 2009b).

### 2.1. Joint control

Each joint is controlled utilizing a two-loop model-following control structure (Osypiuk et al., 2006) assuming an identified nonlinear second order model for each joint (La Hera et al., 2009a). Nonlinear friction, including hydraulic valve dynamics, is compensated for by a model-based addition to the control signal. The joint actuation is controlled using a discretized PID control structure. There are physical constraints on velocity and acceleration in each joint, which have been identified from experiments.

## 2.2. Cartesian control

With inverse kinematics the end-effector motion in cartesian space can be translated into joint velocities. An approach similar as in Mohamed and Chevallereau (1993) and Beiner and Mattila (1999) is taken. The cartesian end-effector velocity can be the momentarily targeted velocity from operator inputs or a pre-planned trajectory. The kinematic structure implies a relation  $\mathbf{p} = f(\theta)$  between the cartesian end-effector position  $\mathbf{p}$  and the joint variables. The end-effector velocity is thus related to the joint velocities as

$$\dot{\mathbf{p}} = \mathbf{J} \dot{\theta} \quad (1)$$

where  $\mathbf{J} = \partial f / \partial \theta$  is the Jacobian of size  $3 \times n$  and the dot symbol represent derivative with respect to time  $t$ . Since the manipulator is kinematically redundant ( $n > m$ ) the Jacobian is in general not invertible and has infinitely many solutions. The pseudo-inverse method provides the solution

$$\dot{\theta} = \mathbf{J}^\dagger \dot{\mathbf{p}}, \quad \text{where } \mathbf{J}^\dagger = \mathbf{W} \mathbf{J}^T (\mathbf{J} \mathbf{W} \mathbf{J}^T)^{-1}, \quad (2)$$

that minimizes the cost-function  $C(\theta) = (1/2) \dot{\theta}^T \mathbf{W} \dot{\theta}$  with positive definite weighting matrix  $\mathbf{W}$  of dimension  $n \times n$ . Diagonal weighting matrix  $\mathbf{W} = \text{diag}(w_1, w_2, \dots, w_n)$  is chosen in what follows. The weighting factors are used for regulating how active or passive a joint is, for avoiding joints reaching their limits and for avoiding singularities by regularization of Eq. (2) accomplished by introducing a functional dependency of  $\theta$  in  $\mathbf{W}$ .

## 2.3. Motion planning and motion tracking

There are well-known for generating smooth paths in cartesian space for moving the end-effector from one position to another and avoiding collision with convex geometries (LaValle, 2006). The general problem of finding a path that is optimal with respect to speed or energy consumption is not considered here nor finding paths that are collision-free for the entire manipulator geometry in a space of concave geometries. A time-independent path is represented as a smooth curve  $\mathbf{q}(s)$ , parametrized by the curve length  $s \in [0, l]$ . In practice cubic splines are used. Also in the absence of user interaction the end-effector position  $\mathbf{p}$  does not necessarily follow the path exactly. The nearest position on the path is denoted by  $\mathbf{q}_p = \mathbf{q}(s_p)$  where  $s_p = \arg \min_{s \in [0, l]} \|\mathbf{p} - \mathbf{q}(s)\|$ . From this point a look-ahead point is defined  $\mathbf{q}_\Delta = \mathbf{q}(s_p + \Delta s)$  at a distance  $\Delta s$  from  $s_p$  along the path. See Fig. 2 for an illustration with the notations. The look-ahead distance can be given a functional dependency on the distance from the path,  $\Delta s(\|\mathbf{p} - \mathbf{q}_p\|) \in [s_{min}, s_{max}]$ , for a smoother return. Linear relation between the look-ahead distance  $\Delta s$  and the distance from the path is used. For tracking of the end-effector along a specific path and for a given tracking speed the automation system computes the target velocity  $\dot{\mathbf{p}}_a$  as

$$\dot{\mathbf{p}}_a = v \frac{\mathbf{p} - \mathbf{q}_\Delta}{\|\mathbf{p} - \mathbf{q}_\Delta\|}, \quad (3)$$

where  $v$  is the tracking speed. The tracking speed is increased and decreased smoothly near the end points of a path. The end-effector target velocity is translated into joint velocities by Eq. 2.

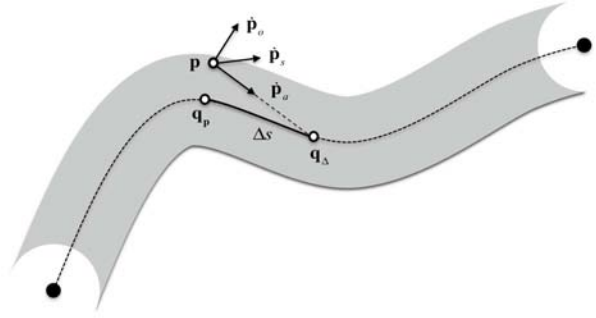


Figure 2: Illustration of path tracking of the end-effector position  $\mathbf{p}$ . Unshaded regions are *weak zones*.

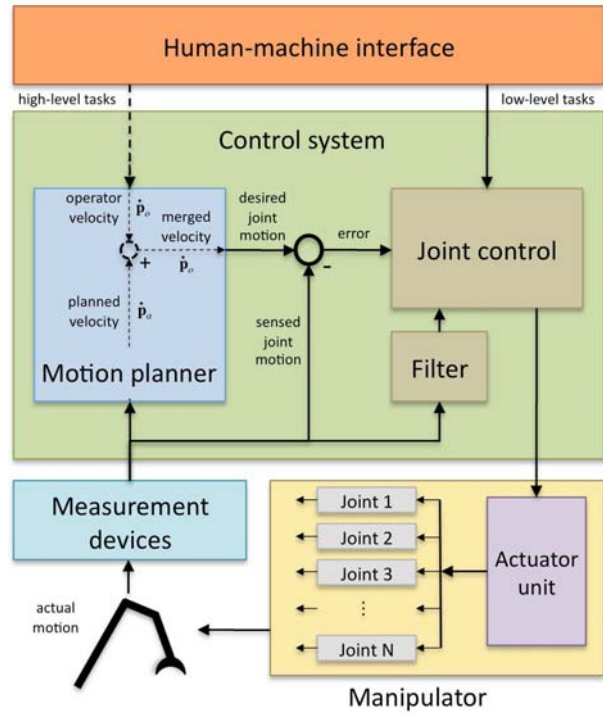


Figure 3: General block diagram for semi-autonomous shared control of a manipulator arm.

## 2.4. Shared control

Shared control between the human operator and the control system is proposed based on mixing the end-effector cartesian velocity references,  $\dot{\mathbf{p}}_o$  and  $\dot{\mathbf{p}}_a$ , respectively. The resulting, merged, velocity reference for shared control is denoted by  $\dot{\mathbf{p}}_s$ . The proposed merging of the velocities are

$$\dot{\mathbf{p}}_s = c_a \dot{\mathbf{p}}_a + c_o \dot{\mathbf{p}}_o, \quad (4)$$

where  $c_a \in [0, 1]$  and  $c_o \in [0, 1]$  are mixing coefficients for decreasing the contribution of  $\dot{\mathbf{p}}_a$  and  $\dot{\mathbf{p}}_o$  to  $\dot{\mathbf{p}}_s$ , respectively. The mixing coefficient  $c_a$  is given functional dependency

$$c_a(\|\dot{\mathbf{p}}_o\|, s_p, \|\mathbf{p} - \mathbf{q}_p\|, t_o) \quad (5)$$

so as to decrease smoothly to zero as the magnitude of the operator reference velocity increases up to a maximal velocity. Furthermore, we propose including functional dependency on the position  $s_p$  along the path, the distance  $\|\mathbf{p} - \mathbf{q}_p\|$  to the path and the time of duration of interaction  $t_o$  is proposed. With this, *weak zones* can be defined, where the contribution from the automation system to the velocity reference can be reduced. Specifically,  $c_a$  reduces monotonically with  $\|\mathbf{p} - \mathbf{q}_p\|$  and on  $t_o$ . The other mixing coefficient can be given functional dependency  $c_o(\mathbf{p}, \dot{\mathbf{p}}_o)$  in order to prevent the operator from running the system into known obstacle geometries, although this is not used in the experiments below. The precise functional dependency on the mixing coefficients, slopes and threshold values, are specific for the geometry of the system, for the application and operator preference. The results in this paper do not depend critically on these values.

The proposed mixing enables simultaneous and shared control between the human operator and computer control system of the end-effector velocity. In the task of tracking a pre-planned motion at a given speed the human operator can chose to stay passive and let the system execute the motion with  $\dot{\mathbf{p}}_s = \dot{\mathbf{p}}_a$  until it has stopped at the end-point. The operator can also chose to interact and change the end-effector velocity in accordance with Eq. (4) and mediated through a suitable mapping from input device signal to operator reference velocity  $\dot{\mathbf{p}}_o$ . This results in a deviation from the pre-planned path. When the operator releases control, i.e.,  $\dot{\mathbf{p}}_o = 0$ , the automation system smoothly regains full control and the end-effector will eventually return to the pre-planned path by Eq. (3). The exception is if the interaction occurred in any *weak zone*, e.g., near the end-point of the path or at distance too far from the path, in combination with large enough operator velocity reference and interaction time in which case  $c_a = 0$  and the control shifts into manual mode permanently,  $\dot{\mathbf{p}}_s = \dot{\mathbf{p}}_o$ , or until a new automation command is executed. This, presumably, result in smooth transitions between autonomous and manual control.

Conventional manual operation is based on operating each joint actuator individually. This is referred to as *joint operation*. This mode may also be requested in combination with semi-autonomous shared control. For this purpose shared control with joint operation is realized as follows. For a given mapping from input device signal to joint velocity references the end-effector cartesian velocity reference is computed by means



Figure 4: The forwarder crane of reduced size at Smart Crane Lab.

of forward kinematics, i.e., Eq. (1). The merged velocity  $\dot{\mathbf{p}}_s$  from Eq. (4) is then translated into joint velocities that are computed using an altered weighting matrix where the weight of the joints activated by the operator is increased while the others are decreased.

## 3. Experiment setup

The methods for semi-autonomous shared motion control presented in previous section have been implemented first in simulator environment and then in lab environment for the purpose of experiments for evaluating the technique. In this section details are given regarding the manipulator and the design of the experiments. The particular application addressed is *forwarding*, i.e., collection and loading of logs. The experiments are designed to produce qualitative measurements relevant for that application. The results should, however, apply for any other application involving similar manipulators and lifting and loading operations of extended objects in unstructured environments.

### 3.1. Manipulator design

The experiments were conducted on a forwarder crane of reduced size at Smart Crane Lab located at Umeå University. The manipulator is shown in Figure 4 and consists of four hydraulic actuated joints – three revolute joints and one prismatic joint – and is equipped with encoders and hydraulic pressure transducers. The crane has a maximum reach of 4.5 m from the base, which is a factor 0.6 of the larger conventional forwarder cranes. For details see La Hera et al. (2009a) and Mettin et al. (2009b). Joint control based on sensor measurements are performed in real-time on a MicroAutoBox (MABX) dSPACE system. The end-effector is a grapple with four degrees of freedom. Opening/closing the grapple is actuated as well as the rotation of the grapple around its axis of symmetry while the remaining two degrees is an unactuated universal joint allowing the grapple to swing. Semi-autonomous control of the grapple rotation is not considered here, although it has been developed (La Hera et al., 2009b). In these experiments the grapple was directly controlled by the operator.

### 3.2. Operator interface

Input devices from a real forest machine is used. This includes a driver seat supplied with two analog joysticks and dig-

ital buttons. The mapping between the motion of the manipulator and the joysticks for joint operation and cartesian operation mode is shown in Figure 5 a) and b), respectively. The mapping for joint control is identical to what is found in real forwarders and the mapping for cartesian operation was designed to resemble this. Next to the joysticks are digital buttons which in these tests are used for giving high-level automation commands.

### 3.3. Experiment design

Experiments are performed with human operators in the loop of controlling the manipulator. The experiments are designed for evaluating the quality of the method for shared control and the effect on operator performance. The operators are given the task to grab and load logs into a target area at high pace avoiding a static obstacle. The loading task can be divided into the sub-tasks *go out* with the grapple to the log, *grab* the log, *go back* to the forwarders target area and *release* the log. The tasks *go out* and *go back* are automated. It is assumed that the operator manually grabs and releases the logs. When the *go out* and *go back* commands are given the system generates a collision free path from the current end-effector position to a pre-defined position centered over the target area or at a fix point in between the two pick-up areas, see Fig. 6. The target area of  $2 \times 1.5$  m is marked by tape on the floor while two symbolic stakes represent the right stakes of the machines load bunk, see Fig. 6. The logs are roughly 1.5 meters long and 0.20 meters in diameter. The operator task is to load four logs into the target area from two pick-up areas. The logs should be loaded one by one in a pre-defined order and must re-oriented to be aligned with the target area. One test series thus includes four work cycles, one for each log. The grapple, with or without log, should go above the static obstacle when moving between the target area and the pick-up areas.

Experiments are conducted with five operators – two professional experienced drivers (O1 and O2) and three novices that are entirely inexperienced in operating a crane (O3, O4 and O5). Before the experiment the professional operators are given some time to be familiarized with cartesian operation and the interface to the semi-autonomous loading system. The novice operators on the other hand will hardly manage the conventional joint operation at the beginning, therefore a training session is designed for the novice operators lasting for approximately one hour and included exercises in joint operation. In the end of the session the novice operators are familiarized with grabbing logs with the grapple, with cartesian operation and the interface to the autonomous sub tasks.

Two operating modes, *joint operation* and *cartesian operation*, are combined with three levels of automation, *manual control*, *traded control* and *shared control* which results in six different operating methods to investigate:

- M1 *manual joint operation* – the operator manually loads the logs with conventional joint operation.
- M2 *traded control alternating with manual joint operation* – the operator alternates between autonomous operation and manual joint operation.

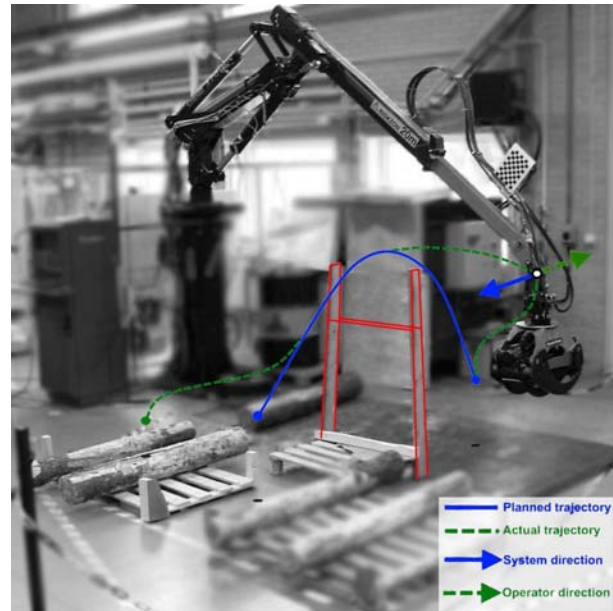


Figure 6: Illustration of *Shared control* between the operator and the autonomous control system in the log loading experiment setting.

- M3 *shared control with manual joint operation* – the operator use autonomous sub-tasks and shared control with manual joint operation.
- M4 *manual cartesian operation* – the operator manually loads the logs with cartesian operation.
- M5 *traded control alternating manual cartesian operation* – the operator use autonomous sub-task control alternated with manual cartesian operation.
- M6 *shared control with manual cartesian operation* – the operator use autonomous sub-task shared control with cartesian operation.

Observe that in traded control mode the operator must wait for the autonomous task ends by decelerating to stop or manually abort it by pushing the abort button. In shared control mode the operator can interact with the autonomous tasks and thereby adjust the path or smoothly take over the control when the automated task is nearly completed whereby the system enters manual operation with no interruptions, see Fig. 6. Spherical weak zones of radius  $\sim 1$  m at the end-point of the paths was used in the experiments.

For each method one test series is made up by the loading of four logs into the target area. Each method is tested in two test series. Hence, each test subject experiment involves twelve test series.

### 3.4. Logging of data

Control signals and information about the operators activity is stored for analysis during all test series. Time stamps are provided each time the end-effector enter or leaves the target

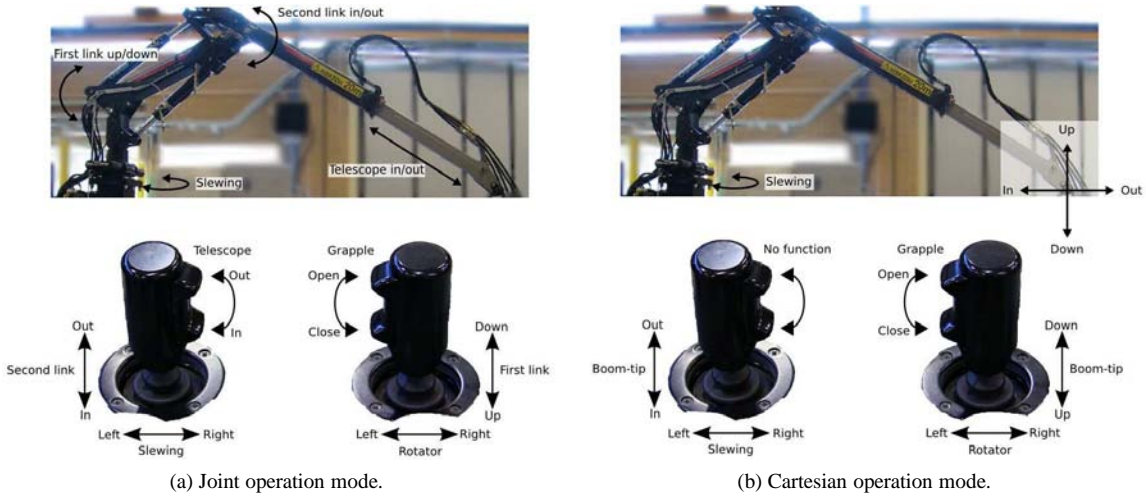


Figure 5: Manual control of crane and grapple.

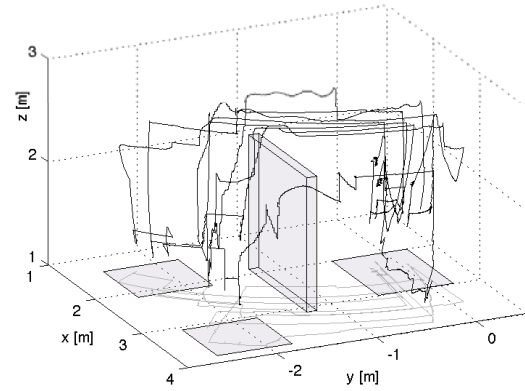
and pick-up areas, defined by a spheres of radius  $1\text{ m}$  centered over the target area. Time stamps for the moments of grabbing and releasing of logs are also logged. From these logs the time spent on each sub-task in each work cycle can be computed as well as the total and average time for the loading cycle. Also positions and velocities are logged for each individual joint and the end-effector. The end-effector velocity is computed from the measured joint positions through forward kinematics. The sampling frequency of the data was  $200\text{ Hz}$ .

#### 4. Results

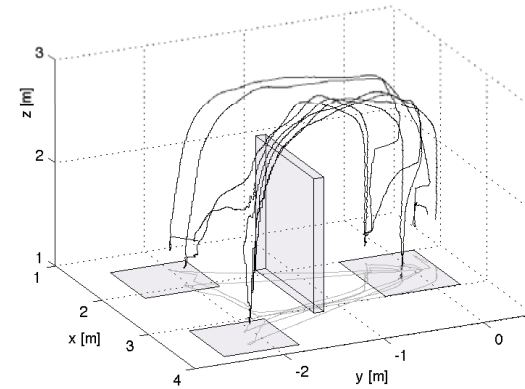
Experiments were conducted to evaluate semi-autonomous shared control with respect to smoothness in the transitions between autonomous and manual control and the effect on operator performance compared to manual and traded control. Sample end-effector trajectories for a novice operator doing log loading using manual joint operation (M1) and semi-autonomous shared control (M6) with cartesian operation is shown in Fig. 7 (a) and (b), respectively. The novice operator has clear difficulties with manual joint operation while semi-autonomous shared cartesian control run much more smoothly.

##### 4.1. Transition smoothness

The system has dynamics on several time-scales,  $\tau$ , that depends on both the system dynamics, the task and the operator behavior. The shortest time-scale is referred to as *noise*. This time-scale,  $\tau < \tau_{noise} \sim 10\text{ ms}$ , is characterized by fluctuations and internal dynamics of the mechanical construction, hydraulics and electronics components. The longest time-scale is that of variations in the end-effector position, velocity etc., when operated smoothly manual,  $\tau > \tau_{smooth} \sim 0.5\text{ s}$ , which is deduced from the characteristic velocity  $1\text{ m/s}$  and characteristic length-scale  $0.5\text{ m}$  of end-effector movements. The intermediate time-scale,  $\tau_{noise} < \tau < \tau_{smooth}$ , consist of undesired oscillations of the manipulator induced by a careless human operator, a swinging load or by deficiencies in the control system.

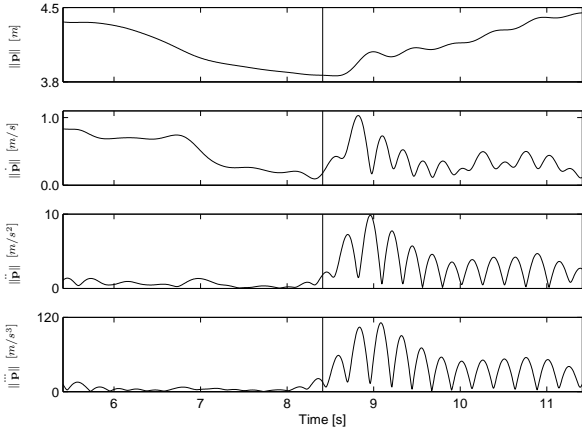


(a) Novice operator with manual joint control (M1).

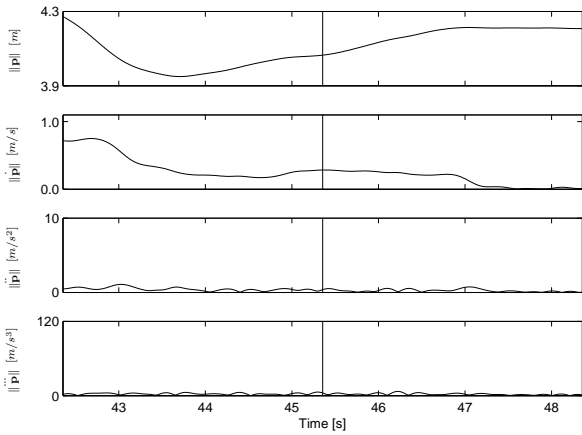


(b) Novice operator with shared cartesian control (M6).

Figure 7: Sample end-effector trajectories.



(a) Sample of non-smooth transition using traded control (M5).



(b) Sample of smooth transition using shared control (M6).

Figure 8: Samples of end-effector position, velocity, acceleration and jerk for transition from autonomous to manual operation.

These oscillations, depending on the magnitude, cause unnecessary wear on the equipment and annoyance and fatigue of the operator.

The smoothness of the end-effector position is studied by analyzing the end-effector trajectory  $\mathbf{p}$ , velocity  $\dot{\mathbf{p}}$ , acceleration  $\ddot{\mathbf{p}}$  and jerk  $\dddot{\mathbf{p}}$ . The noise  $\tau < \tau_{noise} \sim 1$  ms is first removed from the measured trajectories using a low pass filter. The total jerk from time  $t_0$  to  $t_1$  is computed by

$$j = \frac{1}{2} \int_{t_0}^{t_1} (\ddot{\mathbf{p}})^2 dt \quad (6)$$

Filtered sample trajectories of smooth and non-smooth transitions between autonomous and manual operation are shown in Fig. 8 (a) and (b) for a novice operator using traded control (M2) and shared control (M6), respectively. The trajectory with traded control shows a non-smooth transition event with oscillations where the acceleration and jerk peaks of the order of  $10$  m/s<sup>2</sup> and  $100$  m/s<sup>3</sup>, respectively. The corresponding sam-

ple transition with shared control shows smooth behavior with oscillations of a factor 10 smaller in magnitude. Many non-smooth events are also observed in manual joint and cartesian operation by novices. The averaged total jerk for the full loading cycle for each operator and control method is presented in Table 1, normalized with the averaged total jerk  $j = 1570$  m/s<sup>2</sup> for the experienced operators (O1-O2) using manual joint operation (M1) which is the smoothest motion of all. The jerk values ranges from about 1 (smooth) to 10 (very non-smooth). The table shows the clear trend that shared cartesian control (M6) is smooth for both experienced and novice operators, while manual joint operation for novice operators (O3-O5) are the most non-smooth mode. Traded control (M2 and M4) also belong to the more non-smooth modes for both experienced and novice operators. A surprising result is that shared control with joint operation (M3) for experienced operators is more non-smooth than with cartesian operation (M6). Presumably, this means that the weight factors in shared control with joint operation can be tuned more optimally with respect to how the system is expected to respond.

Table 1  
Total jerk in loading cycles

Operator	Mode of operation					
	M1	M2	M3	M4	M5	M6
O1	0.7	4.9	4.1	2.7	4.4	1.8
O2	1.3	2.8	3.5	4.5	2.1	2.0
O3	2.2	4.3	3.9	3.8	3.1	1.8
O4	10.9	7.6	4.3	6.3	4.1	2.9
O5	5.3	9.3	6.3	9.5	3.9	2.2

#### 4.2. Time study

The operator performance is measured by time studies of the task of loading logs. The average time for the loading cycle for experienced and inexperienced drivers for each of the six control methods is listed in figure 9. Figure 10 further includes subtask averages for each individual operator.

As can be seen the performance of the inexperienced operators increases with the level of automation and with the use of cartesian operation rather than joint operation. The inexperienced operators are on average 2.2 times faster using cartesian operation with shared control compared to manual joint operation. Compared to professional operators, the novice operators are more than 3 times slower in conventional joint operation but only a factor 1.3 using semi-autonomous shared control with cartesian operation. From Fig. 10 it is clear that the largest part of the time reduction comes from moving the end-effector from pick-up area to target area. This operation involves coordinating the arm simultaneously with the gripper orientation and avoiding the obstacle. It should, however, be noticed that with semi-autonomous control the performance of the professional drivers is decreased by a factor 1.2. Considering that professional operators has years of training in manual operation, one might expected that with training in semi-autonomous operation the performance may be equally well or even better than with manual operation.

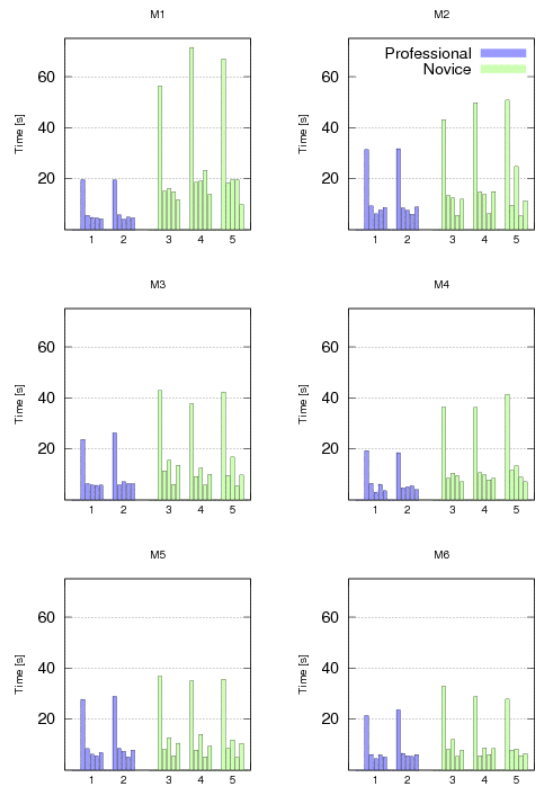
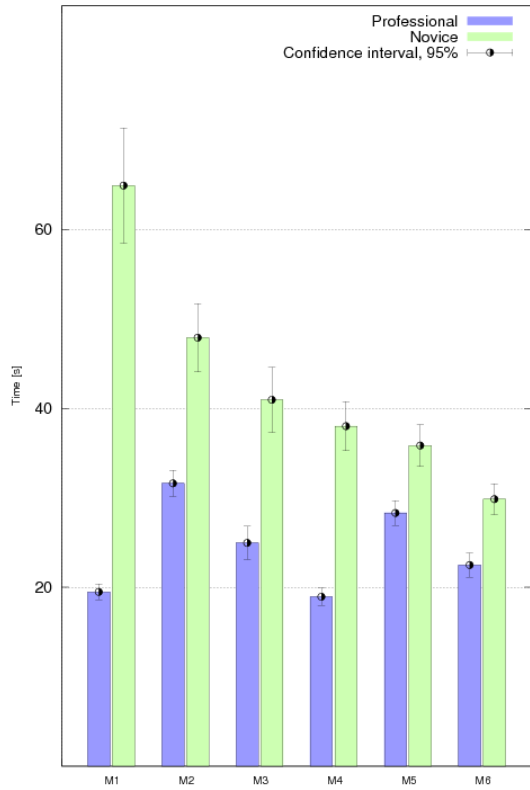


Figure 9: Work cycle average for professional and novice operators.

Figure 10: Work cycle average and subtask average for each individual operator. Subtasks are in the order: *go out from the target area, grab logs, go back to the target area and release logs.*



### 4.3. Operator experience

The operators were also asked to fill out a survey form directly after the tests with questions and gradings regarding the experience of using the different operation modes. Inexperienced operators find cartesian operation much more intuitive. The experienced operators find the precision of cartesian operation to be lower as compared to using joint operation. Both professional and inexperienced operators feel that autonomous tasks reduces the workload, e.g., through that the small pauses in the operators work cycle introduced by autonomous sub-tasks can be used to concentrate on the next pile of logs and on moving and positioning the forwarder.

## 5. Conclusion

This paper presents development and examination of semi-autonomous operation with shared control between the human operator and computer control system of a large-scale kinematically redundant manipulator for gripping and lifting heavy objects in unstructured dynamical environments. The technique is based on mixing of the end-effector velocity references from the human operator and computer control system in combination with robust solutions for inverse kinematics and low-level joint control. The work demonstrates that semi-autonomous operation of heavy large-scale manipulators is feasible and that both inexperienced and professional operators are expected to benefit from it. Smooth shared control enables the human operator to interact and modify pre-planned automated motions. Besides the benefits from reduced workload and increased performance of inexperienced operators the technique can easily be extended to support for novice operators in automatic collision avoidance of known objects and to motion guiding systems, e.g., with force-feedback joysticks.

Future work should examine the effect of the semi-autonomous system on operator fatigue, performance and learning curve during full workdays, e.g., on forwarding systems. A commercial system in rough out-door environments will also require more robust sensor solution than was used in this indoor setting. Model-based open-loop control should then be considered, e.g., with the human operator as a soft sensor.

## 6. Acknowledgements

This work was supported by ProcessIT Innovations and Sparbanksstiftelsen Norrland. The experiments were organized on the equipment of and run using the control algorithms, architecture and support originally developed within the Smart Crane Lab project. Thanks to the volunteer drivers and to the Control System Group at Umeå University for good discussions and assistance.

- Aigner, P., McCarragher, B., 1997. Contrasting potential fields and constraints in a shared control task. In: IROS: 1997 IEEE/RSJ International Conference on Intelligent Robots and Systems.
- Beiner, L., Mattila, J., 1999. An improved pseudoinverse solution for redundant hydraulic manipulators. *Robotica* 17 (2), 173–179.
- Brander, M., Eriksson, D., Löfgren, B., 2004. Automation of knuckleboom work can increase productivity. In: Skogforsk Results, No 4.

- Hallonborg, U., 2003. Förarlösa skogsmaskiner kan bli lönsamma (unmanned forestry machines can be competitive) (in swedish). In: Skogforsk Results, No 9.
- La Hera, P., Mettin, U., Manchester, I., Shiriaev, A., 2008. Identification and control of a hydraulic forestry crane. In: Proceedings of the 17th IFAC World Congress : COEX, South Korea. Elsevier, pp. 2306–2311.
- La Hera, P. X., Mettin, U., Manchester, I., Shiriaev, A., 2009a. Identification and Control of a Hydraulic Forestry Crane. In: Proc. 17th IFAC World Congress, Seoul, Korea.
- La Hera, P. X., Mettin, U., Westerberg, S., Shiriaev, A., 2009b. Modeling and Control of Hydraulic Rotary Actuators used in Forestry Cranes. In: ICRA: 2009 IEEE International Conference on Robotics and Automation.
- Lapointe, J.-F., Robert, J.-M., Boulanger, P., 2001. Optimizing performance in heavy equipment teleoperation. National Research Council Canada – Institute for Information Technology.
- LaValle, S. M., 2006. Planning Algorithms. Cambridge University Press, New York, USA.
- Mettin, U., La Hera, P. X., Morales, D. O., Shiriaev, A. S., Freidovich, L. B., Westerberg, S., 2009a. Trajectory Planning and Time-Independent Motion Control for a Kinematically Redundant Hydraulic Manipulator. In: ICAR: 2009 14th International Conference on Advanced Robotics, Germany. IEEE, pp. 309–314.
- Mettin, U., La Hera, P. X., Westerberg, S., Shiriaev, A., 2009b. Analysis of Human-Operated Motions and Trajectory Replanning for Kinematically Redundant Manipulators. In: IROS: 2009 IEEE/RSJ International Conference on Intelligent Robots and Systems.
- Mohamed, A. A., Chevallereau, C., 1993. Resolution of robot redundancy in the cartesian space by criteria optimization. In: ICRA: 1993 IEEE International Conference on Robotics and Automation. pp. 646–651.
- Osypiuk, R., Kroger, T., Finkemeyer, B., Wahl, F., 2006. A two-loop implicit force/position control structure, based on a simple linear model: theory and experiment. In: ICRA: 2006 IEEE International Conference on Robotics and Automation, Orlando, USA.
- Sheridan, T. B., 1992. Telerobotics, automation, and human supervisory control. MIT Press, Cambridge, MA, USA.
- Tarn, T.-J., Chuanfan Guo, N. X., Wu, Y., 1996. Task-oriented human and machine cooperation in telerobotic systems. *Annual Reviews in Control* 20, 173–178.
- Westerberg, S., Manchester, I. R., Mettin, U., La Hera, P., Shiriaev, A., 2008. Virtual environment teleoperation of a hydraulic forestry crane. In: International Conference on Robotics and Automation, CA, USA. IEEE, pp. 4049–4054.